The specific interaction of the photosensitizer methylene blue with acetylcholinesterase provides a model system for studying the molecular consequences of photodynamic therapy

Israel Silman[a,*], Esther Roth[a], Aviv Paz[a,b,1], Mathilde M. Triquigneaux[c], Marilyn Ehrenshaft[c], Yechun Xu[a,b,2], Valery L. Shnyrov[d], Joel L. Sussman[b], Leesa J. Deterding[e], Yacov Ashani[a], Ronald P. Mason[c], Lev Weiner[f]

[a]Department of Neurobiology, Weizmann Institute of Science, Rehovot 76100, Israel

[b]Department of Structural Biology, Weizmann Institute of Science, Rehovot 76100, Israel

[c]Laboratory of Toxicology and Pharmacology, National Institute of Environmental Health Sciences, National Institutes of Health, Research Triangle Park, NC 27709, USA

[d]Department of Biochemistry and Molecular Biology, Universidad de Salamanca, Salamanca 37007, Spain

[e]Laboratory of Structural Biology, National Institute of Environmental Health Sciences, National Institutes of Health, Research Triangle Park, NC 27709, USA

[f]Department of Chemical Research Support, Weizmann Institute of Science, Rehovot 76100, Israel

[1]Department of Physiology, David Geffen School of Medicine at UCLA, Los Angeles, CA 90095, USA.

[2]Drug Discovery and Design Center, Shanghai Institute of Materia Medica, Chinese Academy of Sciences, Shanghai 201203, China.

Abstract

The photosensitizer, methylene blue (MB), generates singlet oxygen ($^1O_2$) that irreversibly inhibits *Torpedo californica* acetylcholinesterase (*Tc*AChE). In the dark MB inhibits reversibly, binding being accompanied by a bathochromic shift that can be used to show its displacement by other reversible inhibitors binding to the catalytic 'anionic' subsite (CAS), the peripheral 'anionic' subsite (PAS), or bridging them. Data concerning both reversible and irreversible inhibition are here reviewed. MB protects *Tc*AChE from thermal denaturation, and differential scanning calorimetry reveals a ~8 °C increase in the denaturation temperature. The crystal structure of the MB/*Tc*AChE complex reveals a single MB stacked against W279 in the PAS, pointing down the gorge towards the CAS. The intrinsic fluorescence of the irreversibly inhibited enzyme displays new emission bands that can be ascribed to N'-formylkynurenine (NFK); this was indeed confirmed using anti-NFK antibodies. Mass spectroscopy revealed that two Trp residues,

*Corresponding author. fax: +972 8 934 4131. israel.silman@weizmann.ac.il (I. Silman).

Conflict of interest statement
None declared.

Author Manuscript   Author Manuscript   Author Manuscript   Author Manuscript

Trp84 in the CAS, and Trp279 in the PAS, were the only Trp residues, out of a total of 14, significantly modified by photo-oxidation, both being converted to NFK. In the presence of competitive inhibitors that displace MB from the gorge, their modification is completely prevented. Thus, photo-oxidative damage caused by MB involves targeted release of $^1O_2$ by the bound photosensitizer within the aqueous milieu of the active-site gorge.

Keywords

Acetylcholinesterase; Methylene blue; Photosensitizer; Photodynamic therapy; Mass spectroscopy; Singlet oxygen

---

1. Background

Photodynamic therapy (PDT) is being increasingly adopted as a technique for selective local destruction of malignant tumours [1,2]. This treatment involves administration of a photosensitizer, which, upon illumination, generates singlet oxygen ($^1O_2$) that damages biomolecules in its close vicinity, including lipids, proteins and nucleic acids [3]. The photosensitizers currently used in PDT are mostly porphyrins, but they lack specificity for the target cells, and are activated at short wavelengths that generate non-specific damage. These shortcomings can be overcome by using targeted photosensitizers that are excited at longer wavelengths. However, their optimal utilization will require knowledge of their specificity. This, in turn, will necessitate the development of satisfactory model systems.

Methylene blue (MB) (Scheme 1) is a classical photosensitizer that has been utilized for the treatment of a broad spectrum of diseases [4]. It was shown already by Augustinsson that MB serves as a powerful reversible inhibitor of acetylcholinesterase (AChE) in the dark [5], and this interaction was more recently further characterized for both AChE and butyrylcholinesterase (BChE) [6]. Kochevar and coworkers showed that the photosensitizer rose bengal irreversibly inhibited human erythrocyte AChE under illumination [7]. Data concerning both reversible and irreversible inhibition are reviewed below.

In recent years we have utilized *Torpedo californica* AChE (*Tc*AChE) as a model system for studying various types of radiative damage [8–10]. It occurred to us that the tight interaction of MB with *Tc*AChE could provide an ideal experimental system for studying the local oxidative damage produced by $^1O_2$ generated *in situ*, within the active site of a protein.

2. Results

2.1. Reversible inhibition of TcAChE by MB and structural characterization of the MB/TcAChE

As mentioned above, MB is known to serve as a reversible inhibitor of AChE. This was confirmed for *Tc*AChE, using the Ellman assay, with acetylthiocholine as substrate [11]. MB was indeed shown to act as a non-competitive inhibitor of the *Torpedo* enzyme, with $K_i = 33$ nM [12].

In view of the fact that non-specific photoactive damage is wavelength-dependent, we decided to examine the effect of *Tc*AChE on the spectral characteristics of MB. MB itself displays an absorption maximum at 662 nm, and undergoes a bathochromic shift, to 682 nm, upon interaction with the enzyme, with an isosbestic point at 671 nm. Fig. 1 shows an experiment in which MB was titrated with increasing levels of *Tc*AChE until saturation had been achieved. The pronounced bathochromic shift permitted us to monitor the displacement of bound MB by a series of competitive inhibitors for which both the kinetic characteristics and X-ray structural data for their complexes with the enzyme were known [12]. Such data were obtained, in particular, for an inhibitor specific for the 'anionic' subsite of the catalytic site (CAS) at the bottom of the active-site gorge, edrophonium (EDR), for one specific for the peripheral 'anionic' site (PAS) at the entrance to the gorge, propidium (PROP), and for the gorge-spanning bifunctional ligand, BW284c51 (BW), that bridges the CAS and the PAS [13,14]. Both the CAS- and PAS-directed inhibitors could displace the MB from the gorge, but full displacement could only be achieved by using the two together, or by an excess of BW.

In general, reversible inhibitors stabilize *Tc*AChE against thermal denaturation [15]. Fig. 2A shows the pronounced protection against thermal denaturation afforded by MB, and Fig. 2B shows Differential Scanning Calorimetry (DSC) scans in the absence and presence of the ligand [12]. From these scans it can be calculated that in the MB/*Tc*AChE complex, relative to the free enzyme, there is a significant increase in the activation energy of denaturation, E_A (from 74.4 to 146.8 kcal mol^{-1}), and the transition temperature also increases (from 42.6 to 47.9 °C). Furthermore, Fig. 2B clearly demonstrates that the cooperativity of the transition is enhanced.

The crystal structure of the MB/*Tc*AChE complex was obtained by soaking the ligand into crystals of the native enzyme followed by data collection at a synchrotron source [12]. The crystal structure reveals a single molecule of MB bound at the PAS, where it is stacked against the conserved tryptophan residue, Trp279. However, it is oriented along the gorge, towards the active site, in keeping with the observation that the CAS inhibitor, EDR, can displace it from the active-site gorge (Fig. 3).

2.2. Irreversible inactivation of TcAChE by MB under illumination and biophysical characterization of the photo-oxidized protein

Exposure of *Tc*AChE to illumination by white light in the presence of MB resulted in rapid irreversible inactivation [16]. Inactivation occurred at a similar rate if light at wavelengths below 600 nm was cut off by a filter. When the experiment was conducted in deuterated buffer, pronounced enhancement of the rate of inactivation was observed, supporting a mechanism that involves the action of $^1O_2$ generated by the bound MB [17].

Circular dichroism (CD) spectroscopy of the photo-inactivated *Tc*AChE revealed a slight reduction in ellipticity in the far UV, and somewhat increased binding of the amphiphilic probe, 1-anilino-8-naphthalenesulfonic acid (ANS). These findings indicated that photo-oxidation had produced limited unfolding of the protein. However, both ellipticity in the near UV and intrinsic fluorescence were substantially reduced, suggesting photo-oxidative damage to tryptophan residues [16]. Like other partially unfolded species of

*Tc*AChE [18,19], the species generated by photo-oxidation displayed enhanced sensitivity to proteolysis.

In the presence of reversible inhibitors photo-inactivation was retarded, and, conversely, it was shown that photo-oxidation damaged the binding sites for these inhibitors [16].

2.3. Chemical characterization of the photo-oxidized TcAChE

Together with the decrease in intrinsic fluorescence due, apparently, to photo-oxidation of tryptophan residues we observed the appearance of novel emission peaks that could be ascribed to *N*-formylkynurenine (NFK) [20]. Direct evidence to support this contention was obtained by the use of anti-NFK antibodies [21,23] (Fig. 4).

*Tc*AChE contains 14 Trp residues [22]. In order to identify those Trps that had been photo-oxidized in the presence of MB bound specifically within the active-site gorge, proteolytic digestion was followed by mass spectrometric analysis of the peptides generated [23]. This analysis identified peptides bearing the NFK derivatives of Trp84 and Trp 279, present at the CAS and PAS, but not of any other Trp residues (Scheme 2). Furthermore, peptides containing these NFK derivatives were not detected when illumination was performed in the presence of competitive inhibitors that had been shown to displace MB from the active-site gorge.

3. Discussion

The molecular nature of the damage to proteins caused by PDT is obviously a very important issue. It has been demonstrated that $^1O_2$ acts, in particular, on tryptophan, tyrosine, histidine, methionine and cysteine [24], but no experiments have been performed in which its action on a specific protein has been characterized both functionally and structurally. We have utilized *Tc*AChE, which forms a tight complex with the potent photosensitizer, MB, as a model system for approaching this issue.

The crystal structure of the MB/*Tc*AChE complex clearly shows the photosensitizer to be bound within the active-site gorge of the enzyme. It is stacked against Trp279, the principle residue in the PAS, at the top of the gorge, and is oriented down the gorge axis towards the CAS.

It is of interest that while both the structural and kinetic data that we present suggest that *Tc*AChE does not readily form a ternary complex with MB and EDR, such a complex is indeed formed with human AChE [25,26]. Although the 3D structures of *Tc*AChE and human AChE are practically overlapping [27], there are dramatic differences in their rates of reaction with certain covalent inhibitors [28,29] that may arise out of differences in their dynamics. Also, it should be noted that F330, whose orientation in the MB/*Tc*AChE complexes appears to preclude binding of EDR at the CAS, is replaced by a Tyr residue (Y337) in the human enzyme.

The striking result of our study is that of the 14 Trp residues in *Tc*AChE, only the two Trp residues in the two 'anionic' sites, *viz.*, Trp84 in the CAS, and Trp279 in the PAS, are substantially photo-oxidized to NFK. W233, which is at a similar distance (13.1 Å) from

the bound MB as Trp84 (13.8 Å; Fig. 5), is not significantly modified. However, inspection of the crystal structure of *Tc*AChE reveals that, whereas the indole ring of Trp84 faces into the active-site gorge, and indeed interacts with the quaternary groups of thiocholine and of transition-state analogs [30,31], that of Trp233 faces away from the gorge. It is plausible that the $^1O_2$ generated by the photosensitizer can interact with targets within the aqueous milieu. This is in agreement with molecular dynamics simulations which indicated that diffusion of $^1O_2$ generated by the phototoxic fluorescent protein KillerRed occurs preferentially within a water-filled channel [32].

References

[1]. Moan J, Peng Q, An outline of the hundred-year history of PDT, Anticancer Res. 23 (2003) 3591–3600. [PubMed: 14666654]

[2]. Dolmans DE, Fukumura D, Jain RK, Photodynamic therapy for cancer, Nat. Rev. Cancer 3 (2003) 380–387. [PubMed: 12724736]

[3]. Ogilby PR, Singlet oxygen: there is indeed something new under the sun, Chem. Soc. Rev. 39 (2010) 3181–3209. [PubMed: 20571680]

[4]. Oz M, Lorke DE, Hasan M, Petroianu GA, Cellular and molecular actions of methylene blue in the nervous system, Med. Res. Rev. 31 (2011) 93–117. [PubMed: 19760660]

[5]. Augustinsson K-B, Methylene blue as an inhibitor of acetylcholine-esterase, Acta Chem. Scand. 4 (1950) 536–542.

[6]. Küçükkilinç T, Ozer I, Multi-site inhibition of human plasma cholinesterase by cationic phenoxazine and phenothiazine dyes, Arch. Biochem. Biophys. 461 (2007) 294–298. [PubMed: 17428437]

[7]. Allen MT, Lynch M, Lagos A, Redmond RW, Kochevar IE, A wavelength dependent mechanism for rose bengal-sensitized photoinhibition of red cell acetylcholinesterase, Biochim. Biophys. Acta 1075 (1991) 42–49. [PubMed: 1892865]

[8]. Weiner L, Kreimer D, Roth E, Silman I, Oxidative stress transforms acetylcholinesterase to a molten-globule-like state, Biochem. Biophys. Res. Commun. 198 (1994) 915–922. [PubMed: 8117296]

[9]. Weiner L, Roth E, Mazur Y, Silman I, Targeted cross-linking of a molten globule form of acetylcholinesterase by the virucidal agent hypericin, Biochemistry 38 (1999) 11401–11405. [PubMed: 10471290]

[10]. Weik M, Ravelli RBG, Kryger G, McSweeney S, Raves ML, Harel M, Gros P, Silman I, Kroon J, Sussman JL, Specific chemical and structural damage to proteins by synchrotron radiation, Proc. Natl. Acad. Sci. USA 97 (2000) 623–628. [PubMed: 10639129]

[11]. Ellman GL, Courtney KD, Andres V Jr., Featherstone RM, A new and rapid colorimetric determination of acetylcholinesterase activity, Biochem. Pharmacol. 7 (1961) 88–95. [PubMed: 13726518]

[12]. Paz A, Roth E, Ashani Y, Xu Y, Shnyrov VL, Sussman JL, Silman I, Weiner L, Structural and functional characterization of the interaction of the photosensitizing probe methylene blue with *Torpedo californica* acetylcholinesterase, Protein Sci. 21 (2012) 1138–1152. [PubMed: 22674800]

[13]. Harel M, Schalk I, Ehret-Sabatier L, Bouet F, Goeldner M, Hirth C, Axelsen PH, Silman I, Sussman JL, Quaternary ligand binding to aromatic residues in the active-site gorge of acetylcholinesterase, Proc. Natl. Acad. Sci. USA 90 (1993) 9031–9035. [PubMed: 8415649]

[14]. Felder CE, Harel M, Silman I, Sussman JL, Structure of a complex of the potent and specific inhibitor BW284C51 with *Torpedo californica* acetylcholinesterase, Acta Crystallogr. D 58 (2002) 1765–1771. [PubMed: 12351819]

[15]. Weiner L, Shnyrov VL, Konstantinovskii L, Roth E, Ashani Y, Silman I, Stabilization of *Torpedo californica* acetylcholinesterase by reversible inhibitors, Biochemistry 27 (2009) 563–574.

[16]. Weiner L, Roth E, Silman I, Targeted oxidation of *Torpedo californica* acetylcholinesterase by singlet oxygen, Photochem. Photobiol. 87 (2011) 308–316. [PubMed: 21155827]

[17]. Merkel PB, Nilsson R, Kearns DR, Deuterium effects on singlet oxygen lifetimes in solutions – new test of singlet oxygen reactions, J. Am. Chem. Soc. 94 (1972) 1030–1031.

[18]. Dolginova EA, Roth E, Silman I, Weiner LM, Chemical modification of *Torpedo* acetylcholinesterase by disulfides: appearance of a "molten globule" state, Biochemistry 31 (1992) 12248–12254. [PubMed: 1333796]

[19]. Millard CB, Shnyrov VL, Newstead S, Shin I, Roth E, Silman I, Weiner L, Stabilization of a metastable state of *Torpedo californica* acetylcholinesterase by chemical chaperones, Protein Sci. 12 (2003) 2337–2347. [PubMed: 14500892]

[20]. Pirie A, Fluorescence of N'-formylkynurenine and of proteins exposed to sun light, Biochem. J. 128 (1972) 1365–1367. [PubMed: 4674628]

[21]. Ehrenshaft M, Silva SO, Perdivara I, Bilski P, Sik RH, Chignell CF, Tomer KB, Mason RP, Immunological detection of *N*-formylkynurenine in oxidized proteins, Free Radical Biol. Med. 46 (2009) 1260–1266. [PubMed: 19353782]

[22]. Sussman JL, Harel M, Frolow F, Oefner C, Goldman A, Toker L, Silman I, Atomic structure of acetylcholinesterase from *Torpedo californica*: a prototypic acetylcholine-binding protein, Science 253 (1991) 872–879. [PubMed: 1678899]

[23]. Triquigeneaux MM, Ehrenshaft M, Roth E, Silman I, Ashani Y, Mason RP, Weiner L, Deterding LJ, Specific oxidation of *Torpedo californica* acetylcholinesterase by singlet oxygen: identification of *N*-formylkynurenine tryptophan derivatives within the active-site gorge of its complex with the photosensitizer methylene blue, Biochem. J. 448 (2012) 83–91. [PubMed: 22888904]

[24]. Michaeli A, Feitelson Y, Reactivity of singlet oxygen towards amino acids and peptides, Photochem. Photobiol. 59 (1994) 284–289. [PubMed: 8016206]

[25]. Harel M, Sonoda LK, Silman I, Sussman JL, Rosenberry TL, Crystal structure of thioflavin T bound to the peripheral site of *Torpedo californica* acetylcholinesterase reveals how thioflavin T acts as a sensitive fluorescent reporter of ligand binding to the acylation site, J. Am. Chem. Soc. 130 (2008) 7856–7861. [PubMed: 18512913]

[26]. Wildman SA, Zheng X, Sept D, Auletta JT, Rosenberry TL, Marshall GR, Drug-like leads for steric discrimination between substrate and inhibitors of human acetylcholinesterase, Chem. Biol. Drug Des. 78 (2011) 495–504. [PubMed: 21668653]

[27]. Kryger G, Harel M, Giles K, Toker L, Velan B, Lazar A, Kronman C, Barak D, Ariel N, Shafferman A, Silman I, Sussman JL, Structures of recombinant native and E202Q mutant human acetylcholinesterase complexed with the snake-venom toxin fasciculin-II, Acta Crystallogr. D Biol. Crystallogr. 56 (2000) 1385–1394. [PubMed: 11053835]

[28]. Kraut D, Goff H, Pai RK, Hosea NA, Silman I, Sussman JL, Taylor P, Voet JG, Inactivation studies of acetylcholinesterase with phenylmethylsulfonyl fluoride, Mol. Pharmacol. 57 (2000) 1243–1248. [PubMed: 10825396]

[29]. Bar-On P, Millard CB, Harel M, Dvir H, Enz A, Sussman JL, Silman I, Kinetic and structural studies on the interaction of cholinesterases with the anti-Alzheimer drug rivastigmine, Biochemistry 41 (2002) 3555–3564. [PubMed: 11888271]

[30]. Harel M, Quinn DM, Nair HK, Silman I, Sussman JL, The structure of a transition state analog complex reveals the molecular origins of the catalytic power and substrate specificity of acetylcholinesterase, J. Am. Chem. Soc. 118 (1996) 2340–2346.

[31]. Colletier J-P, Fournier D, Greenblatt HM, Sussman JL, Zaccai G, Silman I, Weik M, Structural insights into the catalytic pathway of acetylcholinesterase, EMBO J. 25 (2006) 2746–2756. [PubMed: 16763558]

[32]. Roy A, Carpentier P, Bourgeois D, Field M, Diffusion pathways of oxygen species in the phototoxic fluorescent protein KillerRed, Photochem. Photobiol. Sci. 9 (2010) 1342–1350. [PubMed: 20820672]
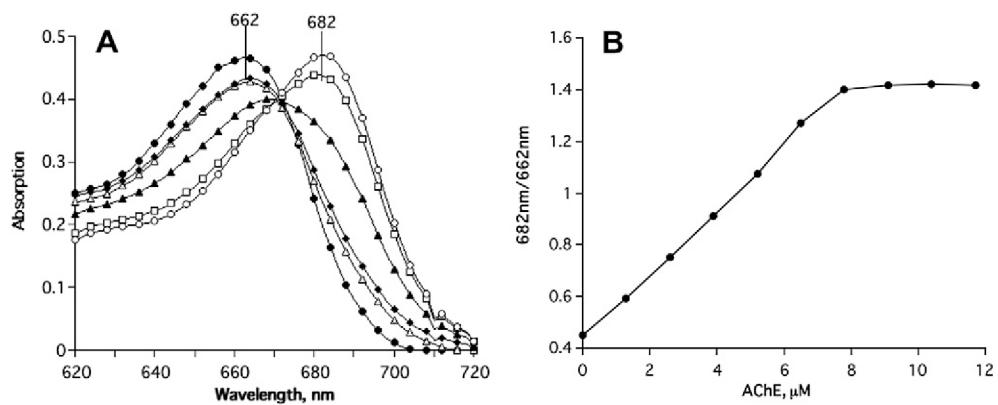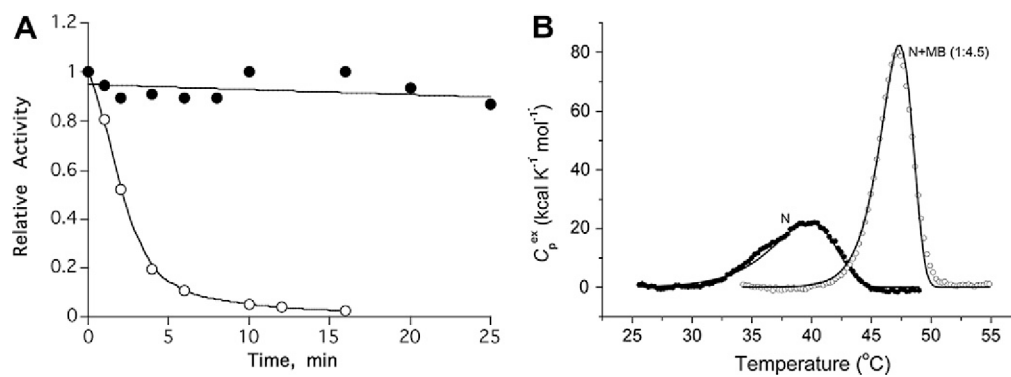
Fig. 1.
Monitoring of the bathochromic shift in the absorption maximum of MB produced by its interaction with *Tc*AChE. (A) Shift in the absorption maximum upon titration of 5 μM MB with increasing concentrations of *Tc*AChE; (B) saturation curve calculated on the basis of data similar to those shown in (A) [12].

Fig. 2.
(A) Protection by MB of *Tc*AChE against thermal inactivation. O-O-O, incubation of 1.5 μM *Tc*AChE at 39 °C; ●-●-●, 1.5 μM *Tc*AChE + 50 μM MB at 39 °C [12]. (B) Temperature-dependence of the excess molar heat capacity of *Tc*AChE (N) and of the MB/ *Tc*AChE complex (N + MB) at a scan rate of 60 K h^{-1} in 0.1 M NaCl/10 mM HEPES, pH 7.5. Solid lines represent the best fit for each experimental curve to a simple two-state model of protein denaturation [12].
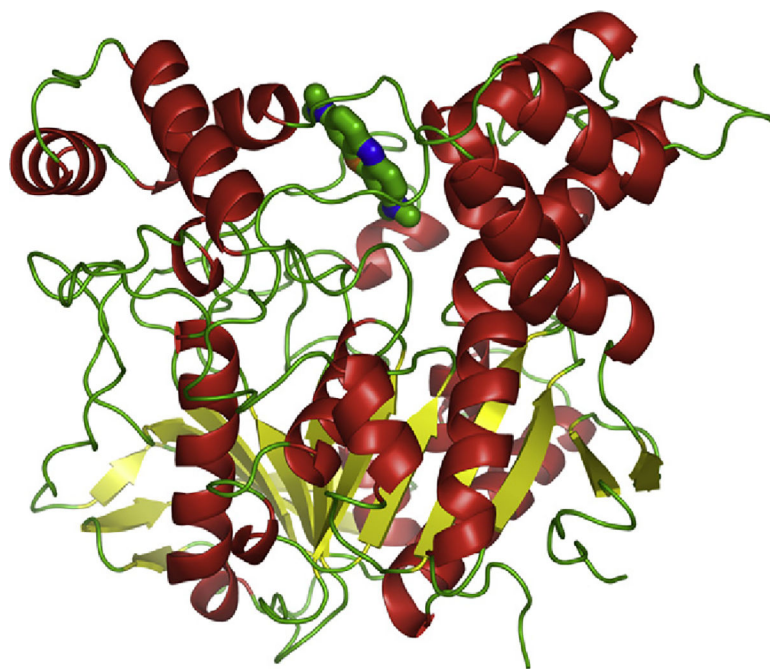
Fig. 3.
Crystal structure of the MB/*Tc*AChE complex. Cartoon representation with helices in red, sheets in yellow, loops in green [12]. The MB molecule, in stick representation, is seen at the top of the image at the entrance to the active-site gorge.
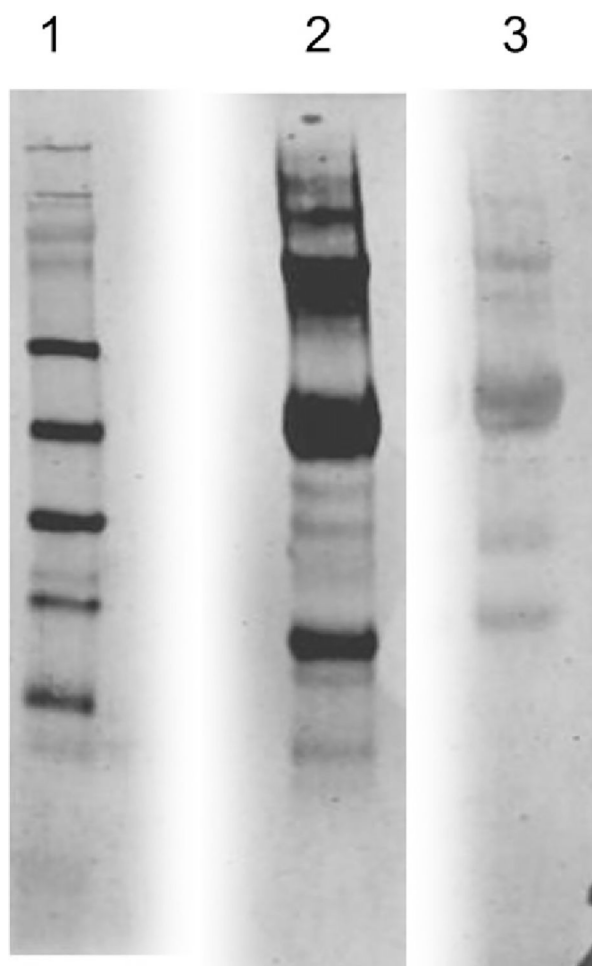
Fig. 4.
Detection of NFK in *Tc*AChE illuminated in the presence of MB. Lane 1, MW markers stained with Coomassie blue; Lane 2, western blot with anti-NFK antibodies of *Tc*AChE illuminated in the presence of MB; Lane 3, western blot with anti-NFK antibodies of *Tc*AChE illuminated in the presence of MB together with the reversible inhibitors, EDR and PROP.

Fig. 5.
Ribbon diagram of the MB/*Tc*AChE complex. MB is color-coded blue. The two Trp residues converted to NFK, Trp279, adjacent to the MB, and Trp 84, are colored magenta, and the remaining Trp residues are in green.
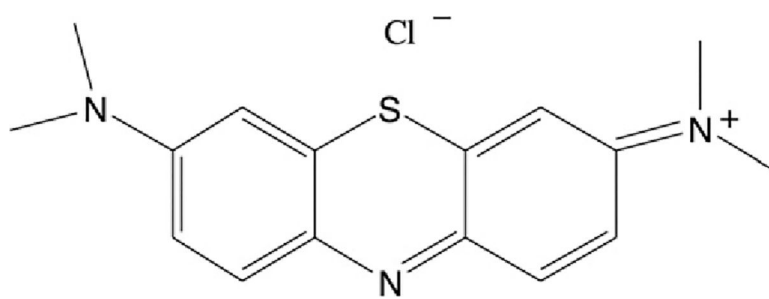
Scheme 1.

^{71}VDEQFPGFSGSEM$_{OX}$W$_{NFK}$NPNREMSEDC$_{CAM}$LY^{96}

^{267}REKKPQELIDVEW$_{NFK}$NVLPF^{284}

Scheme 2.